Supplementary Information

Missing Interstellar Sulfur in Inventories of Polysulfanes and Molecular Octasulfur Crowns

Ashanie Herath[1,2], Mason McAnally[1,2], Andrew M. Turner[1,2], Jia Wang[1,2], Joshua H. Marks[1,2], Ryan C. Fortenberry[3†], Jorge C. Garcia-Alvarez,[4] Samer Gozem[4‡] and Ralf I. Kaiser[1,2]*

[1]Department of Chemistry, University of Hawai'i at Mānoa, Honolulu, HI, USA 96822.

[2]W. M. Keck Laboratory in Astrochemistry, University of Hawai'i at Mānoa, Honolulu, HI, USA 96822.

[3]Department of Chemistry and Biochemistry, University of Mississippi, Oxford, MS, USA 38677.

[4]Department of Chemistry, Georgia State University, Atlanta, GA, USA 30302.

Corresponding authors:

†r410@olemiss.edu, ‡sgozem@gsu.edu, *ralfk@hawaii.edu

Supplementary Note 1

In calculations to find out the isotopic mass distribution of S_8 in mass channels *m/z* = 256 to *m/z* = 260, the natural isotopic distribution of sulfur[1] and permutational equations were utilized. For each mass channel, the contribution from each combination (A) calculated via: $A = \frac{n!}{a!b!c!} {P_1}^a {P_2}^b {P_3}^c$, where n is the total number of atoms in the molecule, a,b,c are the isotopes in the considered permutation, and P_1, P_2, P_3 are the abundances of each isotope. As an example, for *m/z* = 256, only eight of ^{32}S can contribute to *m/z* = 256, thus a 66.4% (0.950^8) of S_8 signal. Similarly, for *m/z* = 257, only possible contributor is $^{32}S_7{}^{33}S$. Contribution of S_8 into the *m/z* =257 via $^{32}S_7{}^{33}S$ can be calculated as $\frac{8!}{7!1!}\times(0.950)^7\times(0.0076)$: 4.25%.

But for *m/z* = 258, two possible contributors of S_8 existing, $^{32}S_6{}^{33}S_2$ and $^{32}S_7{}^{34}S$. Likewise, the contribution of $^{32}S_6{}^{33}S_2$ to *m/z* = 258 would be $\frac{8!}{6!2!}\times(0.950)^6\times(0.0076)^2$: 0.01% and contribution of $^{32}S_7{}^{34}S$ to *m/z* = 258 would be $\frac{8!}{7!1!}\times(0.950)^7\times(0.0422)$: 24.8%. For signal at m/z = 260 from S_8, via $^{32}S_6{}^{34}S_2$ is only a minor contributor with only $\frac{8!}{6!2!}\times(0.950)^6\times(0.0422)^2$: 3.7%.

Supplementary Note 2

In order to calculate approximate amount of S_8 predicted in the TMC, predicted amount of hydrogen, S/H ratio in TMC-1[2] and the product branching ratios reported in this study were utilized. A spherical shape was approximated for the TMC cloud of length 30 pc.[3] Utilizing the predicted hydrogen density $n_H = 2\times10^4$ cm^{-3} and S/H ratio of 1.5×10^{-5}, 1.3×10^{53} atoms/ single sulfur molecules are expected. Incorporating the 3.7% average product yield obtained for S_8 in this study, 2.1×10^{53} kg – or 350 Earth masses – of octasulfur can be expected to be formed in the exposure to the GCRs.

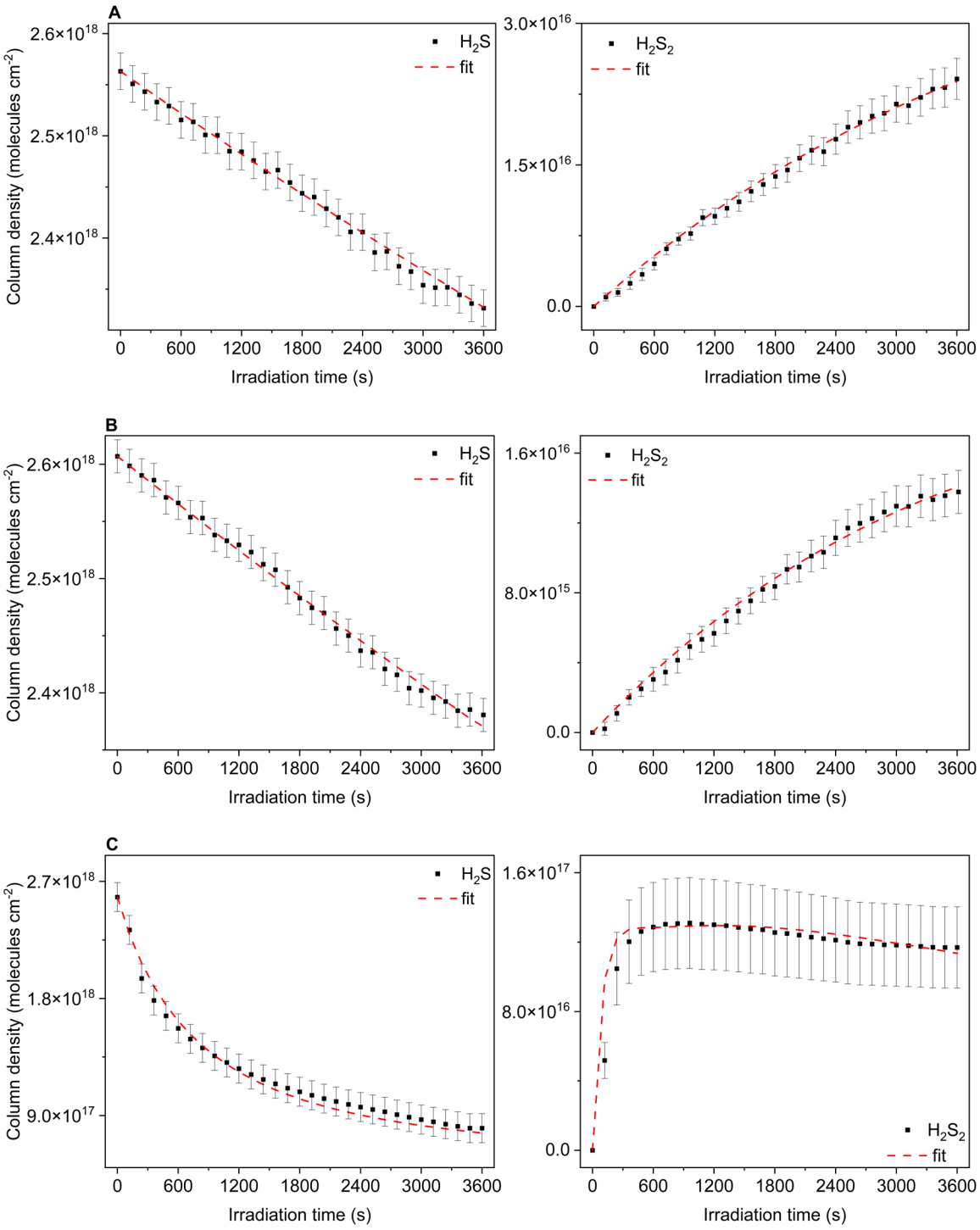

Supplementary Figure 1: Kinetic fits of infrared peak profiles during the irradiation phase. Column densities of hydrogen sulfide (H_2S: *left*) decay and the formation of hydrogen disulfide (H_2S_2: *right*) during the electron irradiation on ices at 5 K at three different doses of irradiation. **A:** 3.6 ± 0.5 eV molecule^{-1}, **B**: 36 ± 1 eV molecule^{-1} and **C:** 180 ± 11 eV molecule^{-1}. Error bars include the instrumental noise and errors in the ice thickness measurements.

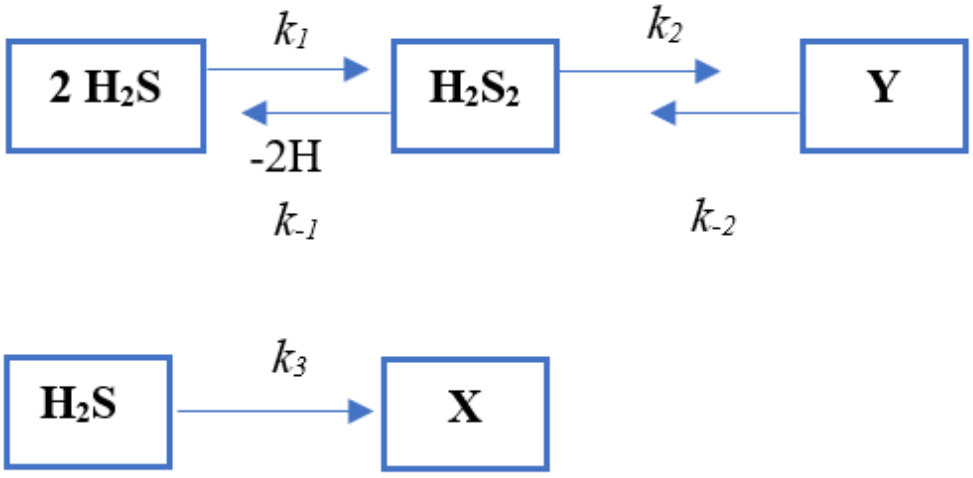

Supplementary Figure 2: Reaction scheme used to fit the temporal profiles of decay and new profiles in the hydrogen sulfide (H_2S) ices at 5 K. The column densities of hydrogen sulfide (H_2S) and dihydrogen sulfide (H_2S_2) were traced in the irradiation phase in every two minutes (Fig. 2) were fitted with coupled differential equations.

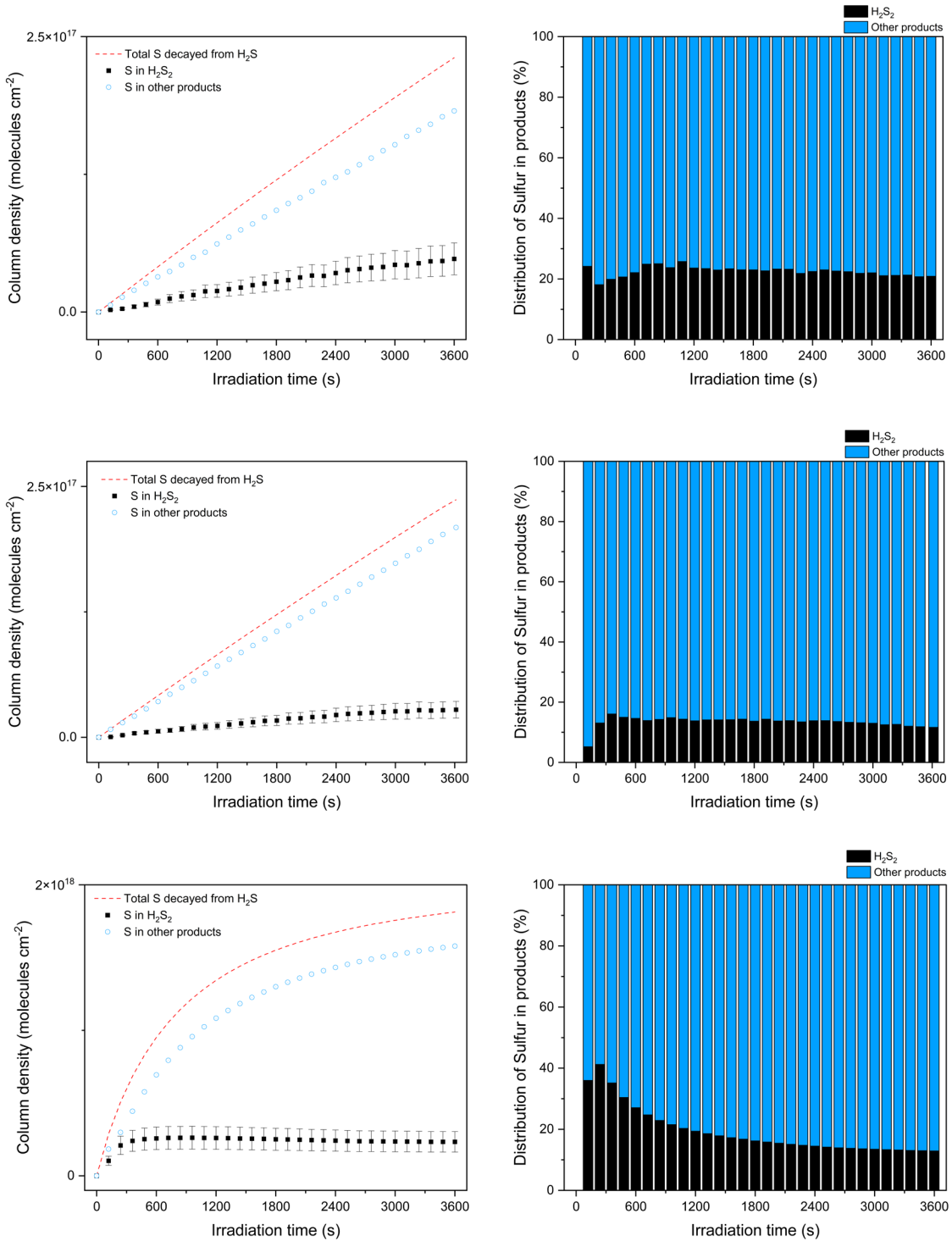

Supplementary Figure 3: Sulfur budget of the irradiated ices between hydrogen disulfide (H_2S_2) and higher order sulfur containing products identified via FTIR in the hydrogen sulfide ices irradiated with the three doses. *Top:* 3.6 ± 0.5 eV molecule^{-1}, *middle:* 36 ± 1 eV molecule^{-1} and *bottom:* 180 ± 11 eV molecule^{-1}.

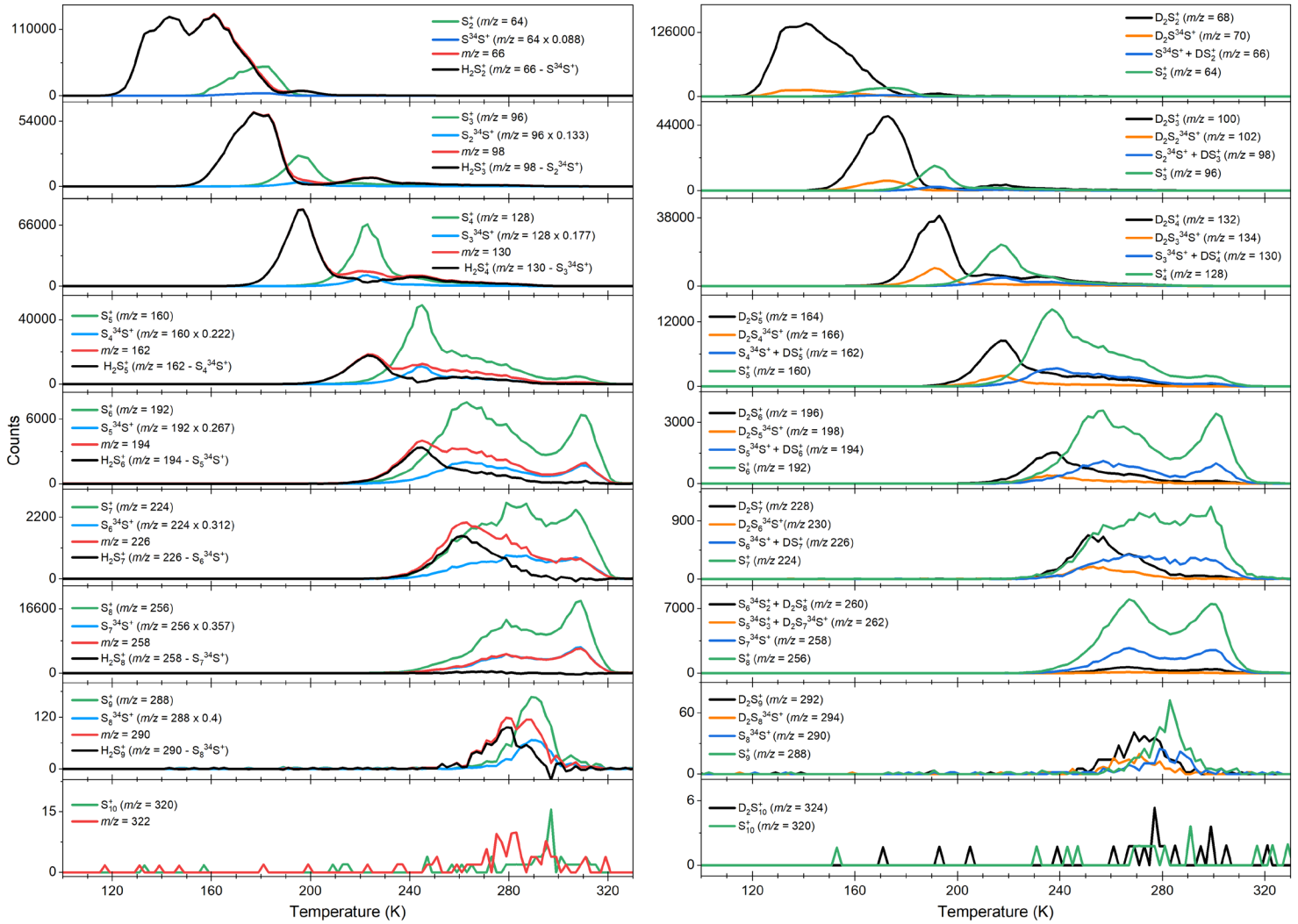

Supplementary Figure 4: Signals observed in ReToF mass spectrometer for sulfanes and the molecular fragments with same number of sulfur atoms subliming at different temperatures for hydrogen sulfide ice (left) and deuterium sulfide ice (right) at 10.49 eV photons. Black lines indicate each sulfane, whereas green lines: sulfur fragments. Deuterated ice confirmed the assigned mass formulae at each mass via a mass shift.

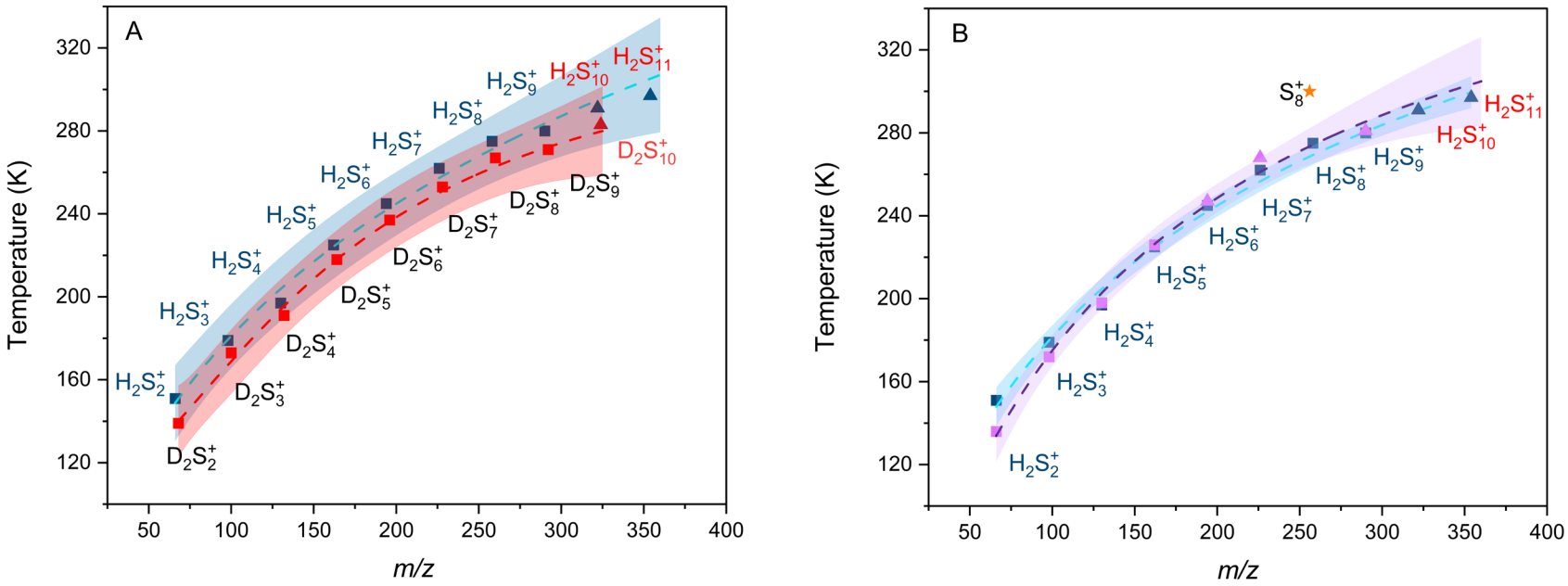

Supplementary Figure 5: Peak sublimation temperatures as a function of the masses of sulfanes and octasulfur. Squares represent the species that were identified via the molecular ions, while triangles represent the species whose sublimation temperatures were indirectly identified using their respective S_{n-1}^+ mass fragments. A) Comparison of sublimation temperatures of sulfanes (*blue,* $H_2S_n^+$; n = 2-11) versus deuterated sulfanes (*red,* $D_2S_n^+$; n = 2-10) observed using PI-ReToF-MS. The sublimation temperatures of observed sulfanes and deuterated sulfanes were used to create the blue and red trendlines. Both trendlines within the error overlap in the predicted ranges. B) Peak sublimation temperatures of sulfanes observed by ReToF-MS (*blue*), and species that were observed in RGA (*violet*) creates blue and violet trendlines that overlap in the predicted error ranges. Yellow star indicates the crown conformers of octasulfur subliming at a distinct sublimation temperature, away from the sublimation temperatures of sulfanes.

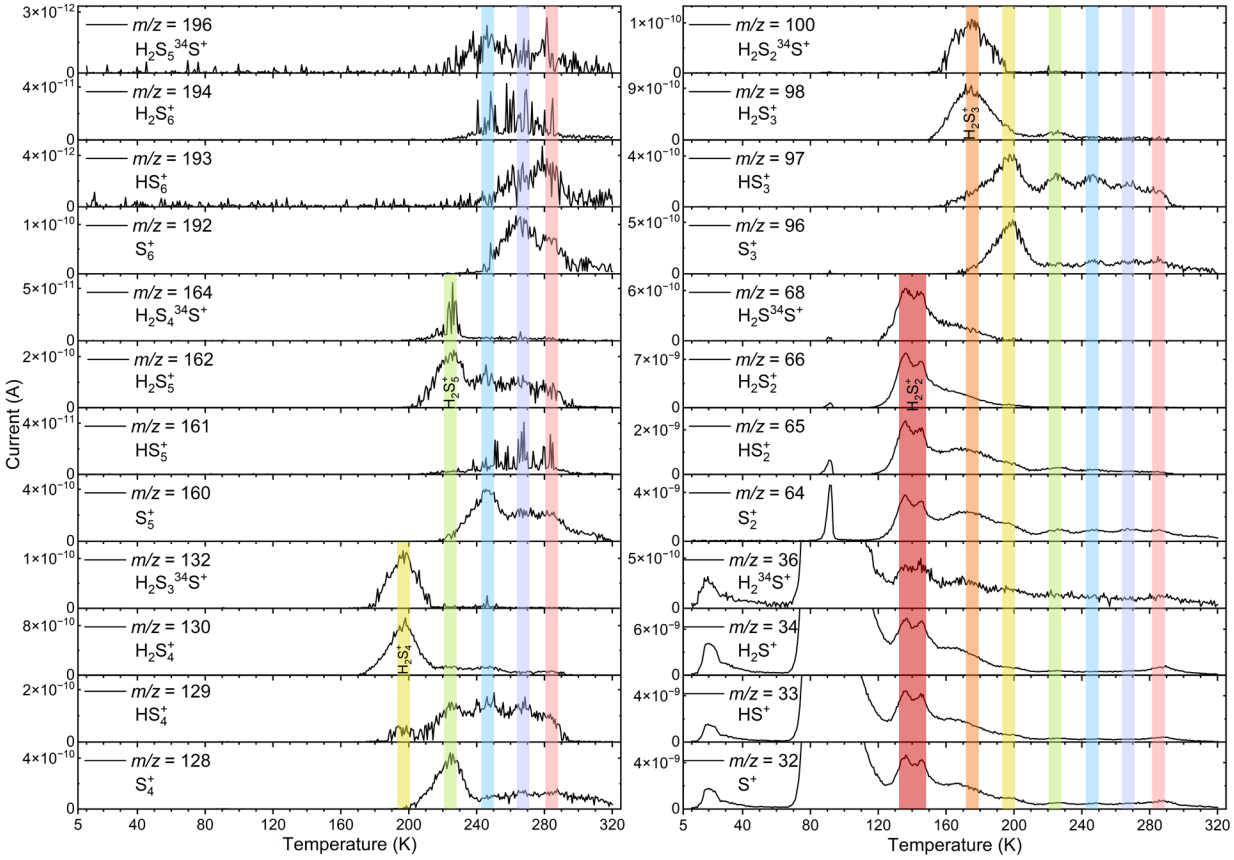

Supplementary Figure 6: TPD profiles for the indicated mass channels observed in the residual gas analyzer (RGA) for the hydrogen sulfide ice. The colored lines connect the sublimation events that take place at the same temperature. Sublimation events indicated by the colored lines red, orange, yellow and green indicate the parent peaks and the observed fragmentation of them. *Red:* $H_2S_2^+$, *orange:* $H_2S_3^+$, *yellow:* $H_2S_4^+$, *green:* $H_2S_5^+$. Fragments along the colored lines blue, purple and pink are projected to be fragments of $H_2S_6^+$ (*blue*), $H_2S_7^+$ (*purple*) and $H_2S_9^+$ (*pink*). The panels of single sulfur species are zoomed in to show the fine peaks after the sublimation of H_2S centered around 90 K.

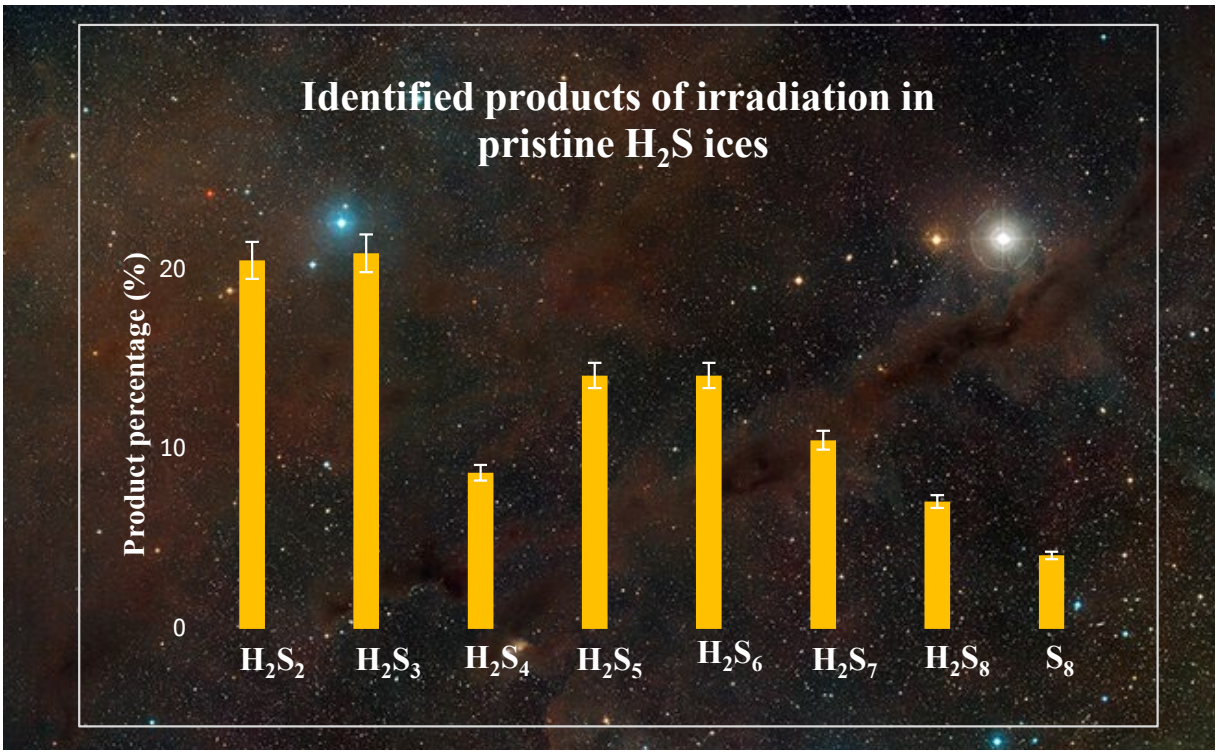

Supplementary Figure 7: Irradiation products of the hydrogen sulfide ice identified via PI-ReToF-MS. Indicated errors include errors in theoretical calculations, ice thickness measurements and in dose calculations.

Supplementary Table 1: Infrared absorption assignments for hydrogen sulfide ice before irradiation and the formed products after electron irradiation.

Assignment	Position (cm^{-1})	References
Before irradiation (10 K)		
$\nu_2 + \nu_1$ / ν_3	3711	[4,5]
ν_1 / $\nu_3 + \nu_T$	2650	[5]
ν_1 / ν_3	2552	[5]
ν_2	1169	[4,5]
New peaks from irradiation		
H_2S_2 (ν_5)	2482	[6]
$H_2S_{n\ ;(n=2-5)}$ (ν(SH))	2443	[7]

Supplementary Table 2: Rate constants calculated for each irradiation dose experiment via the solutions of coupled differential equations for the reaction scheme in Fig. S1.

Rate constant, k	3.6 ± 0.5 eV molecule^{-1}	36 ± 1 eV molecule^{-1}	180 ± 11 eV molecule^{-1}	Reaction order
k_1	$1.5 \pm 0.1 \times 10^{-24}$ [a]	$9.3 \pm 0.2 \times 10^{-24}$ [a]	$2.3 \pm 0.1 \times 10^{-22}$ [a]	Second order
k_2	$1.5 \pm 0.2 \times 10^{-4}$ [b]	$2.2 \pm 0.3 \times 10^{-4}$ [b]	$7.6 \pm 0.2 \times 10^{-3}$ [b]	First order
k_3	$2.0 \pm 0.5 \times 10^{-5}$ [b]	$2.2 \pm 0.5 \times 10^{-5}$ [b]	0	First order
k_{-1}	0	0	$1.5 \pm 0.2 \times 10^{-3}$ [b]	First order
k_{-2}	0	0	$1.9 \pm 0.3 \times 10^{-3}$ [b]	First order

[a]Units: cm^2 $molecules^{-1}$ s^{-1}. [b]Units: s^{-1}.

Supplementary Table 3: Error analysis of adiabatic ionization energies (IEs) and relative energies of distinct S_8 isomers. IEs and relative energies were calculated with F12-TZ//B3LYP/aug-cc-pVTZ levels of theory including zero-point vibrational energy corrections. The IE ranges are corrected for the thermal and Stark effect by–0.03 eV and the combined error limits of –0.08/+0.02 eV.

	S_8 isomer	Structure	*m/z*	Relative energy (kJ mol^{-1})	IE (eV)	IE range with error (eV)	Corrected IE with Stark effect (eV)
1	Crown/ twisted	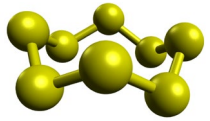	256	0.0	8.85 ± 0.05	8.80 – 8.90	8.77 – 8.87
2	Chair	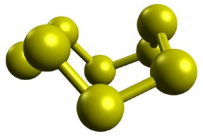	256	39.1	8.20 ± 0.05	8.15 – 8.25	8.12 – 8.22
3	C_{2h}	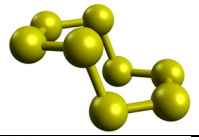	256	67.6	8.26 ± 0.05	8.21 – 8.31	8.18 – 8.28
4	Boat	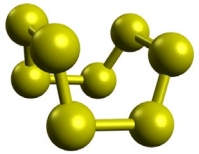	256	69.0	8.30 ± 0.05	8.25 – 8.35	8.22 – 8.32
5	Cluster chain	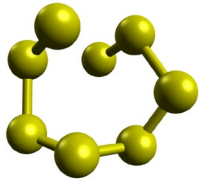	256	70.0	8.61 ± 0.05	8.56 – 8.66	8.53 – 8.63
6	S_7S	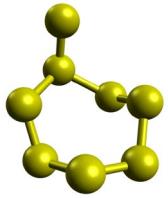	256	108.8	8.31 ± 0.05	8.26 – 8.36	8.23 – 8.33

Supplementary Table 4: Parameters used in irradiation dose calculations for the experiments on hydrogen sulfide ices.

Initial kinetic energy of electrons, k eV	5.0			
Density of ice, g cm^{-3}	1.1			
Total molecules irradiated, molecules	$(2.6 \pm 0.5) \times 10^{18}$			
Thickness of ice, nm	1330 ± 50			
Average penetration depth, nm	350 ± 30			
Fraction of transmitted energy, eV	0.000			
Irradiated area, cm^2	1.6 ± 0.1	3.2 ± 0.3		
Irradiation currents, nA	100	100	1000	5000
Total number of electrons	$(2.3 \pm 0.1) \times 10^{15}$	$(2.3 \pm 0.1) \times 10^{15}$	$(2.25 \pm 0.05) \times 10^{16}$	$(1.12 \pm 0.06) \times 10^{17}$
Dose per molecule of H_2S, eV $molecule^{-1}$	7 ± 1	3.6 ± 0.5	36 ± 1	180 ± 11

Supplementary Table 5: Photoionization experiments utilize four wave mixing schemes to generate vacuum ultraviolet (VUV) photons. At least one dye laser pumped by a neodymium yttrium-aluminum garnet (Nd:YAG) laser was used with appropriate harmonic (355 or 532 nm) in accordance with the dye.

Medium	ω_{VUV}	Nd:YAG Wavelength (nm)	ω_1 (nm)	ω_1 dye	Nd:YAG Wavelength (nm)	ω_2 (nm)	ω_2 dye	Energy (eV)
Krypton	$2\omega_1 - \omega_2$	355	202.316	Rhodamine 610/640 mix	532	863.0	LDS 867	10.82
Xenon	$3\omega_1$	355[a]	-	-	-	-	-	10.49
Krypton	$2\omega_1 - \omega_2$	355	212.556	Stilbene 420	532	532[a]	-	9.34
Krypton	$2\omega_1 - \omega_2$	355	212.556	Stilbene 420	355	479.438	Coumarin 480	9.08
Xenon	$2\omega_1 - \omega_2$	355	222.566	Coumarin 450	532	532[a]	-	8.81
Krypton	$2\omega_1 - \omega_2$	355	212.556	Stilbene 420	-	425.112	-	8.75
Xenon	$2\omega_1 - \omega_2$	355	222.566	Coumarin 450	355	442.596	Coumarin 450	8.34
Krypton	$2\omega_1 - \omega_2$	355	212.556	Stilbene 420	355	355[a]	-	8.17

[a]Nd:YAG harmonic

Supplementary Table 6: Photoionization cross sections calculated for the sulfanes H_2S_2 to H_2S_8 and octasulfur (S_8).

	Ionization energy (eV)	Calculated photoionization cross sections (Mb)							
		8.17 eV	8.34 eV	8.75 eV	8.81 eV	9.08 eV	9.34 eV	10.49 eV	10.82 eV
H_2S	10.45	0	0	0	0	0	0	14.8 ± 8.1	17.2 ± 6.9
H_2S_2	9.05	0	0	0	0	18.5 ± 9.8	20.0 ± 8.0	23.8 ± 4.8	24.5 ± 4.6
H_2S_3	9.00	0	0	0	0	12.2 ± 6.1	13.3 ± 5.5	17.8 ± 3.0	18.9 ± 2.5
H_2S_4	8.70	0	0	29.1 ± 15.4	29.9 ± 15.1	33.4 ± 13.3	36.5 ± 11.9	46.7 ± 9.1	49.0 ± 8.5
H_2S_5	8.66	0	0	26.5 ± 11.9	27.2 ± 11.5	30.3 ± 10.1	33.1 ±9.0	44.0 ± 6.6	46.6 ± 6.8
H_2S_6	8.65	0	0	35.1 ± 22.3	36.2 ± 21.9	40.9 ± 19.7	44.7 ±18.3	55.5 ± 15.9	57.6 ± 15.1
H_2S_7	8.60	0	0	32.3 ± 15.6	33.2 ± 15.3	37.4 ± 14.3	41.1 ±13.8	54.0 ± 14.0	57.0 ± 13.9
H_2S_8	8.67	0	0	33.1 ± 16.5	34.0 ± 15.7	38.2 ± 12.1	41.6 ±9.5	52.7 ± 5.5	55.5 ± 5.2
S_8	8.85	0	0	0	0	31.6 ± 22.7	34.0 ±19.6	39.6 ± 14.2	40.4 ± 13.1

1 Mb = 1×10^{-18} cm^2

References:

1. Macnamara, J. & Thode, H. G. Comparison of the Isotopic Constitution of Terrestrial and Meteoritic Sulfur. *Phys. Rev.* **78**, 307–308 (1950).
2. Navarro-Almaida, D. *et al.* Gas phase Elemental abundances in Molecular cloudS (GEMS): II. On the quest for the sulphur reservoir in molecular clouds. On H_2S case. *Astron. Astrophys.* **637**, (2020).
3. Güdel, M. *et al.* The XMM-Newton extended survey of the Taurus molecular cloud (XEST). *Astron. Astrophys.* **468**, 353–377 (2007).
4. Salama, F. *et al.* The 2.5-5.0μm spectra of Io: evidence for H_2S and H_2O frozen in SO_2. *Form. Stars planets, Evol. Sol. Syst. Proc. 24th ESLAB Symp. Friedrichshafen, 1990* **2**, 203–208 (1990).
5. Fathe, K., Holt, J. S., Oxley, S. P. & Pursell, C. J. Infrared spectroscopy of solid hydrogen sulfide and deuterium sulfide. *J. Phys. Chem. A* **110**, 10793–10798 (2006).
6. Zengin, N. & Giguère, P. A. Infrared spectrum of crystalline H_2S_2. *Can. J. Chem.* **37**, 632–634 (1959).
7. Cazaux, S. *et al.* Photoprocessing of H_2S on dust grains. *Astron. Astrophys.* **657**, A100 (2022).